Energy Conversion and Management: X 23 (2024) 100646

Contents lists available at ScienceDirect

Energy Conversion and Management: X

journal homepage: www.sciencedirect.com/journal/energy-conversion-and-management-x

Energy, exergy, environmental and economy (4E) analysis of the existing of biomass-ORC plant with capacity 150 kWe: A case study

Diki Ismail Permana [a,b,c,*], Federico Fagioli [b], Maurizio De Lucia [b], Dani Rusirawan [c], Istvan Farkas [d]

[a] Doctoral School of Mechanical Engineering, Hungarian University of Agriculture and Life Science, Godollo 2100, Hungary
[b] Dipartemento di Ingegneria Industriale, Universita Degli Studi Di Firenze, Florence 50139, Italy
[c] Department of Mechanical Engineering, Institut Teknologi Nasional Bandung, Bandung 40123, Indonesia
[d] Institute of Technology, Hungarian University of Agriculture and Life Science, Godollo 2100, Hungary

ARTICLE INFO

Keywords:
Biomass
Organic Rankine cycle
Bologna
Economy
Sustainability

ABSTRACT

Biomass makes a substantial contribution to Italy's renewable energy mix. In 2018, 19,235 GWh of energy were created, continuing a trend that began three years earlier. Italy's demand for biofuel is expected to reach 2.8 million tonnes of oil equivalent by 2025 and remain constant until 2040. Biomass combustion frequently generates high temperatures (900–1000 °C), which justifies the construction of high-temperature heat recovery units such as steam Rankine or supercritical carbondioxide (SCO2) cycles. However, these methods are only economically practical on a medium to large scale. Small-scale units have high component costs because of the high specific volume of steam, while high turbomachinery costs mostly hamper small sCO2 systems. So, another alternative way is to use an organic Rankine cycle (ORC). This study uses thermodynamic analysis to determine how much power can be achieved in terms of energy, exergy, economy and what impact on sustainability is achieved at the Bologna ORC plant. From the study results, it was found that the Bologna unit has a capacity of 150 kWe. When data was collected, the maximum power obtained was 85 kW at a temperature and pressure of 153 °C and 1.84 MPa, respectively. Biomass-ORC investment is economically competitive, with NPV and LCOE values of 238 kE and 0.93 E/kWh, respectively, and a simple payback period of 24 years for residents with yearly energy needs of 2000 h.

Introduction

Italy is one of the largest electricity producing countries in Europe, around 10 % less than Germany and France. Currently, the use of renewable energy sources in Italy is greater (40.2 %) than the average for European Union (EU) countries (32.9 %) in 2018 [1]. 280 TWh was produced in Italy, while the remaining 43.9 TWh was imported from several neighboring countries. Italy was formerly energy-independent, but since the early 1980 s, demand has begun to outstrip output. The disparity has been relatively steady over the previous two decades. This was worsened by the impact of the Russia-Ukraine war since Italy heavily relied on Russian natural gas supplies in 2021, accounting for over 40 % of total gas imports (72.6 billion standard/m^3). In 2022, Italy reduced its Russian gas imports by half (to 19 % of the total) while increasing exports threefold [2].

According to Terna, the Italian power grid operator, electricity consumption in 2022 was 317 TWh; as in 2021, national production covered 86.4 % of the need, with the remainder coming from imported electricity. Nonrenewable thermoelectric power generation climbed by 7.9 %, accounting for 64.8 % of total output (48.8 % natural gas, 9.1 % solid fuels, and 6.9 % petroleum products and other fuels). Renewable electricity generation declined from 35.3 % to 30.6 %, accounting for approximately 19 % of total energy consumption. For the first time, due to lesser precipitation, solar-generated electricity equaled hydroelectric power (about 28 %). The remaining part came from wind (20.7 %), biomass (17.4 %), and geothermal (5.5 %). Electricity imports climbed by 1.8 %, while exports grew by 16.4 % [3]. Even though renewable energy sources from solar and wind are relatively high, these energy sources are greatly influenced by weather factors. Thus, the use of biomass becomes an alternative source of renewable energy. Biomass contributes significantly to Italy's renewable energy contribution. In 2016, biomass and waste-based energy output reached 19.378 TWh, up from 10.832 TWh in 2011. In 2018, 19,235 GWh of energy was

* Corresponding author at: Doctoral School of Mechanical Engineering, Hungarian University of Agriculture and Life Science, Godollo 2100, Hungary..
E-mail address: permana.diki.ismail@phd.uni-mate.hu (D.I. Permana).

https://doi.org/10.1016/j.ecmx.2024.100646
Received 20 March 2024; Received in revised form 19 May 2024; Accepted 12 June 2024
Available online 13 June 2024
2590-1745/© 2024 The Author(s). Published by Elsevier Ltd. This is an open access article under the CC BY-NC license (http://creativecommons.org/licenses/by-nc/4.0/).

Nomenclature

C_{ash}	Annual ash disposal cost
C_{bio}	Annual biomass consumption cost
C_e	Annual electricity net selling price
C_h	Annual heating net selling price
$C_{O\&M}$	Annual operational cost and maintenance
C_p	Specific heat at pressure constant (J/kg.K)
C_{ncf}	annual revenues and operational costs
C_{TCI}	system's total capital investment
e_x	Exergy specific (kJ/kg)
$\dot{E}_D$	Exergy destruction (kJ)
$\dot{E}_X$	Exergy (kJ)
$\dot{EX}^Q_{in}$	Exergy heat input (kJ)
$\dot{EX}^Q_{out}$	Exergy heat ouput (kJ)
g	Gravitational acceleration (9.8 m/s^2)
h	Specific enthalpy (kJ/kg)
i	Intereset rate
ln	Logaritma natural
$\dot{m}$	Mass flow rate (kg/s)
$\dot{m}_w$	Mass flow rate of cooling water (kg/s)
n	Project lifettime
P	Pressure (Pa)
P_{crit}	Critical pressure (MPa)
P_0	Pressure at dead state (MPa)
$\dot{Q}$	Heat (W)
R	Universal gas constant (8.3154 J/mol.K)
s	Specific entropy (kJ/kg.K)
$\dot{S}_{gen}$	Rate of entropy generation
T	Temperature (°C)
T_0	Temperature at dead state (°C)
$T_{h,i}$	Temperature of heat input (°C)
$T_{h,o}$	Temperature of heat output (°C)
V	Velocity of fluid (m^3/s)
$\dot{W}_{pump}$	Work on pump (W)
$\dot{W}_{expander}$	Work on expander (W)
$\dot{W}_{net}$	Work net (W)

Greek symbols

β	Influence coefficient
γ	Density
€	Euro currency
η	Efficiency
ψ	Exergy efficiency
Σ	Summation
ν	Degree thermodynamic perfection

Subscripts

ava	available
avg	average
bio	biomass
cond	condenser
crit	critical
evap	evaporator
ex	exergy
exp	expander
h	heat
in	Inlet
loss	losses
net	netto
out	outlet
pump	pump
thermal	thermal
use	usable
wf	Working fluid
0	dead state

Abbreviation

ASHRAE	American Society of Heating Refrigerating and Air Conditioning Engineers
EEF	Environmental Effect Factor
ESI	Exergy Sustainability Index
EU	European Union
EWR	Exergy Waste Ratio
GWP	Global Warming Potential
HHV	High Heating Value
HVAC	Heating Ventilating and Air Conditioning Engineers
LCOE	Levelized Cost of Electricity
LHV	Low Heating Value
NIST	National Institute of Standard and Technology
NPV	Net Present Value
ODP	Ozone Depletion Point
ORC	Organic Rankine Cycle
PCM	Phase Change Material
PV	Photovoltaic
SCO2	Supercritical Carbon dioxide
SIC	Specific Investment Cost
SPB	Simple Payback Period

generated, following a consistent trend over the previous three years. Italy's demand for biofuel is predicted to reach 2.8 million tonnes of oil equivalent in 2025 [4] and stay stable until 2040.

Biomass refers to biodegradable products, waste, and leftovers from agriculture, forestry, and associated sectors and the biodegradable part of industrial and municipal waste [5]. Forest biomass accounts for 70 % of energy recovery feedstock. In contrast to the global trend, the area of European woods is steadily expanding. This makes European forest biomass a viable resource. Agricultural and waste biomass provides 30 % of the total supply [6]. Therefore, In Italy, forests and woodlands occupy 110 x 103 km^2, or 36.5 % of the national territory [7]. Only 18 % of the forest surface is planned or managed. These findings highlight forests as an underutilised resource. Using this potential amount in cogeneration facilities with a work capacity of 4000 h/y and acceptable efficiency can result in a potential power of 1900 MWel, with an extra electrical output of 7.5 TWh and thermal production of 30 TWh [8].

Biomass combustion often produces high temperatures (about 900–1000 °C), justifying the development of units for high-temperature heat recovery such as steam Rankine or sCO2 cycles [9]. However, both systems are only economically feasible at medium to large scales. Small scale units have high component costs due to the high specific volume of steam, but tiny sCO2 systems are mainly penalised by high turbomachinery costs [10]. Furthermore, several researchers have studied the use of biomass not only as an electricity generator but as a hybrid [11] of gasification [12], solar [13], district heating and cooling for household or industrial use [14,15] and biofuel production [16]. Therefore, Gimeli and Luongo [17], investigated the issue thermodynamically and experimentally in a biomass power plant with a capacity of 2.3 MW, obtaining low plant efficiency due to the small size, biomass supply range, and continual fluctuation in the operating point.

It has been mentioned above that the use of biomass ultimately requires high temperatures and a large scale, which only some regions in Italy can afford. So, another alternative way is to use an organic Rankine cycle (ORC). ORC works based on the Rankine generator in general, and

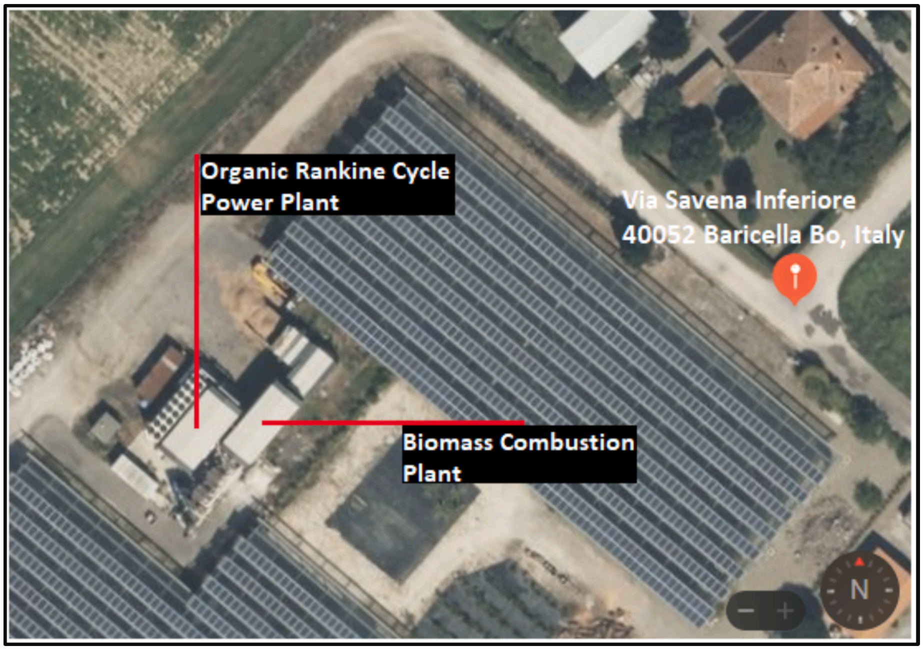

Fig. 1. Location of Baricella Biomass-ORC Plant.

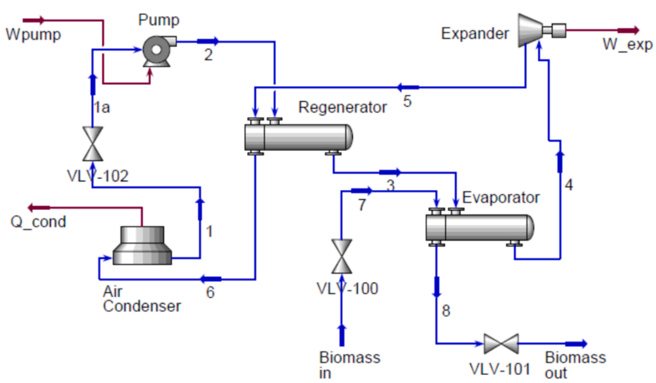

Fig. 2. The simple schematic diagram of biomass-ORC plant.

the refrigerants or mixtures fluid is used as the working fluid that has a lower boiling point than water with low ODP and GWP. So, generating electricity on a small scale at lower temperatures (>200 °C) and using residual biomass is very possible. Moreover, some components of ORC generation may use HVAC or chiller components. Furthermore, many researchers have studied and developed ORC systems from various alternative heat sources such as solar [18–21], geothermal brine [22,23], industrial or residual heat.

Based on ORC map.org [24], 430 projects or 330 GW of biomass-ORC capacity spread worldwide have been installed over the last 15 years. Meanwhile, the most significant number of biomass-ORC projects are on the European continent, and the largest country is Italy, with 23 projects. However, for installed capacity, Germany ranks first with 125 GWe.

Few studies have explored using ORC to recover heat from biomass combustion waste at mid to high temperatures. Georgousopoulos et al. [25] evaluated the thermodynamics and economics of combining an ORC with an integrated gasification cycle to optimise waste heat recovery across three scenarios. Zeotropic mixes were the most effective working fluid across all three conditions. The proposed systems have a levelized cost of electricity ranging from 35.42 to 35.67 EUR/MWh. Zhang et al. [26] investigated the thermodynamic performance of ORC combined with waste heat recovery from the Rankine, Brayton, and thermoelectric generators. Under five operational situations, we tested R123, R245, and R600 organic fluids. The DORC design was the most efficient when used with the R123, resulting in net output, thermal, and exergy efficiencies of 32.63 kW, 26.55 %, and 54.36 %. Moharamian et al. [27] conducted thermodynamic and exergoeconomic analyses of ORC in combination with biomass-integrated co-firing and post-firing technologies, which use a combination of natural gas and biomass as feedstock, as well as externally fired technology that only uses biomass. After testing several fluids, including R141b, R123, n-Pentane, HFE7000, and water, researchers found that R141b has the highest thermal and exergy efficiencies but is the least cost-effective option. Oyekale et al. [28] investigated the cost-effectiveness of retrofitting biomass in hybrid CSP-Biomass ORC power plants, both in constant and modular modes. The study focused on an operational CSP-ORP installation in Ottana, Itlay, comprising linear Fresnel collectors, two thermal oil storage tanks, and a 630 kW ORC unit. The study found that retrofitting with biomass improves electrical efficiency by 5 % and can boost operational hours by up to 3500. The proposed technique has a payback period of 1.4 years, with an LCOE of 109 GBP/MWh and a net present value of GBP 1.83 million.

Many researchers have optimized and improved the performance of ORCs in many applications. ORCs have been extensively explored for their thermodynamic, economic, and environmental benefits in recovering waste heat from diverse operations. So, in this paper, we report an experimental ORC study based on the existing biomass-ORC through energy, exergy, environmental and economy (4E) analysis.

Methodology

System description

Fig. 1 shows the biomass-ORC is in 4052 Baricella (Latitude: N 44° 38′ 33.076″, Longitude: W 11° 31′ 23.162″), the region is 15 km from the city of Bologna, Italy. The capacity of the plant is 150 kWe using R134a working fluid. The temperature and pressure from wood waste combustion are around 160–180 °C with 11–12 bar, respectively. This study used Microsoft Excel combined with NIST Refprop to carry out calculations assisted by Unisim software as a comparison application.

Figs. 2 and 3 are diagrams of the ORC cycle using a regenerator and T-s diagram of the biomass-ORC process represented by R134a working

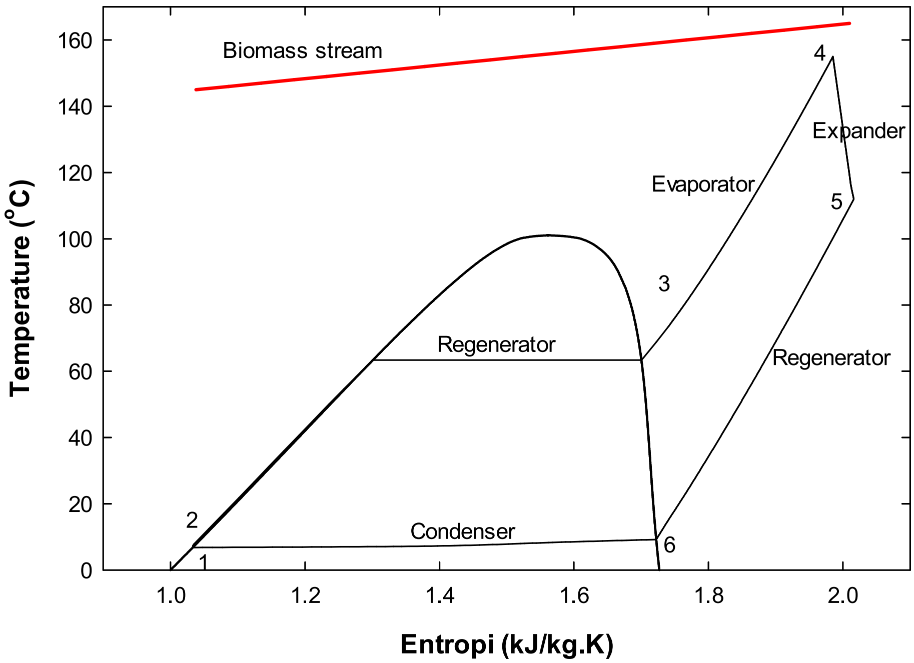

Fig. 3. The process statement of biomass-ORC using R134a.

Table 1
The properties of R134a [31].

Property	unit	value
Critical density ($\rho_{critical}$)	Kg/m^3	511.9
Critical temperature ($T_{critical}$)	°C	101.6
Boiling temperature at 1 atm ($T_{boiling}$)	°C	−26.3
Critical pressure ($P_{critical}$)	MPa	4.0593
ODP	–	0
GWP	–	1300
Toxity	–	n.a
ASHRAE class	–	A1
Molar mass	kg/mol	102.032

Table 2
Physical and chemical properties of woodwaste [32].

Analysis	Biomass content	unit	value
Ultimate analysis	Carbon	%	50.56
	Hydrogen	%	6.70
	Nitrogen	%	0.16
	Sulfur	%	0.20
	Oxygen	%	42.51
	Chlorin	%	0.002
Approximate analysis	Volatile matter content	%	81.81
	Ash	%	0.36
	Fixed carbon	%	17.83
	LHV	kJ/kg	19.74
	HHV	kJ/kg	19.40

fluid, respectively.Hot steam (7) from the Biomass combustion chamber enters the evaporator to transfer heat to the working fluid so that the supercritical phase, with high appropriate pressure and temperature, can enter the expander (4) and produce the appropriate power. The resulting expansion in the expander causes a decrease in pressure and temperature sufficient to preheat the regenerator section (5) so that the work in the evaporator is not too heavy. From the regenerator (6), the working fluid enters an air-cooled condenser to cool and change the phase of the working fluid to a saturated liquid. Hopefully, it becomes a subcooled liquid when it enters the pump (6). The pump is a plunger piston type, capable of increasing the working fluid pressure to 4–5 MPa.

Table 3
Breakdown of purchased components of ORC.

Components Cost	Cost function	reffs
Biomass boiler	$C_{boiler} = 1600(\dot{m}_{biomass} \times 0.9 \times 3600)^{0.67}$	[40]
ORC expander	$C_{ORCexp} = 6000W_{ORCexp}^{0.7}$	[40]
ORC pump	$C_{ORCpump} = 3540W_{ORCpump}^{0.71}$	[41]
ORC evaporator	$C_{ORCevap} = 309.14(A_{ORCevap}) + 293.15$	[41]
ORC regenerator	$C_{ORCreg} = 1.3(190 + A_{ORCreg})$	[41]
air condenser	$C_{ORCcond} = 1397A_{ORCond}^{0.89}$	[42]
Working fluid	$C_{wf} = 25\ \dot{m}_{fluid}$	[42]

Table 4
Break down of non-purchased components [43,44].

Non-component cost	% PEC
Purchased equipment installation	30
Piping	20
Instrumentation and controls	10
Electrical equipment and materials	10
Structural work	15
Engineering and supervision	25
Contingencies	20
Startup and working capital	20
Sum	150

It enters the regenerator (5) to obtain initial heat from the expansion, which results in the expander.

Unisim calculates the physical and chemical characteristics of all programme components based on given pressure and temperature parameters. In addition, additional assumptions are used to simplify the calculation models, which are as follows [29,30]: 1) The suggested system functions under steady-state circumstances, 2) Air and flue gas are considered ideal gases, 3) Neglecting pressure losses in components and pipe lines, 3) the compressor, expander, and pump have constant isentropic efficiencies, 4) The mass flow rate for biomass remains

Table 5
Base-case economic assumptions.

Parameter	Value
Electricity selling price	95 €/MWhe [45]
Ash disposal cost	60 €/tn of ash [46]
Project lifetime (n)	25 years [46]
Annual operation and maintenance	2 % of TCI [47]
Interest rate (i)	7 % [47]
Biomass fuel cost (waste wood) per wet ton	50 €/tn [46]
Biomass consumption	1500 tn/year [46]
Heat selling price	100 €/MWh [48]
Construction	2 years

Table 6
Main parameter and assumption.

Parameter	Unit	Value
P_{cond}	MPa	0.43
$T_{cooling}$	°C	5.1
Pinch point	°C	10
T_{reg}	°C	73.6
$T_{subcooling}$	°C	Calculated
P_{evap}	Mpa	1.84
$T_{expander}$	°C	153
$W_{expander}$	kW	85 (calculated)
W_{pump}	kW	4.8 (calculated)
$\eta_{expander}$	%	70
η_{pump}	%	65
$\dot{m}$	kg/s	2

Table 7
Comparing results of actual condition vs Unisim.

Parameter	Unit	Actual	Unisim	Difference (%)
P_{cond}	MPa	0.43	0.45	4.44
$T_{cooling}$	°C	5.1	5.1	0
T_{reg}	°C	73.6	74.54	1.28
P_{evap}	Mpa	1.84	1.87	1.09
$T_{expander}$	°C	153	155	1.31
$W_{expander}$	kW	85	85.3	0.35
W_{pump}	kW	4.8	3	4.25

constant. Therefore, Table 1 and 2 shows the properties of R134a and woodwaste for biomass combustion, respectively. The R134a working fluid was chosen because it has a low boiling point and is environmentally friendly based on the ODP and GWP values. Not only that, R134a is available on the market and has a price that tends to be cheap compared to other working fluids. Meanwhile, the selection of wood waste has been explained in the introduction based on the raw materials available in Italy, which are pretty abundant.

Energy, exergy and exergy sustainability

The first and second law of thermodynamics should be applied to determine the performance of the ORC. The energy equilibrium equation may be used to calculate the quantity of work generated and the heat required by the ORC. The formula for each component are as follows [33]:

Process 1–2, pump:

$$\dot{W}_{pump} = \frac{\dot{m}(h_1 - h_2)}{\eta_{pump}}, \tag{1}$$

Process 2–3, regenerator:

$$\dot{Q}_{reg} = \dot{m}(h_2 - h_3), \tag{2}$$

Process 3–4, evaporator:

$$\dot{Q}_{evap} = \dot{m}(h_4 - h_3), \tag{3}$$

Process 4–5, expander:

$$\dot{W}_{exp} = \dot{m}(h_4 - h_5)\eta_{exp}, \tag{4}$$

Process 6–1, condenser:

$$\dot{Q}_{cond} = \dot{m}(h_6 - h_1), \tag{5}$$

The net power output of biomass-ORC can be evaluated through the following equation:

$$\dot{W}_{net} = \dot{W}_{exp} - \dot{W}_{pump} \tag{6}$$

Meanwhile, the thermal efficiency is as follows:

$$\eta_{thermal} = \frac{\dot{W}_{net}}{\dot{Q}_{evap}} = \frac{\dot{W}_{exp} - \dot{W}_{pump}}{\dot{Q}_{evap}}, \tag{7}$$

Then, the Eq. (8) for calculating the biomass mass flowrate in the evaporator:

$$\dot{m}_{bio} = \frac{\dot{Q}_{evap}}{\eta_{global} LHV_{bio}} \tag{8}$$

where $\dot{m}_{bio}$ is the biomass mass flowrate (kg/s), η_{global} is the global efficiency of the boiler (%); LHV_{bio} is the low heating value of biomass (kJ) and the value is obtain from Table2.

Furthermore, an exergy balance for the biomass-ORC system is performed to assess total energy in terms of the first and second thermodynamic principles. In a steady state condition, exergy balancing may be described as follows: i is the rate of exergy destruction, $\dot{m}_{ex}$ is the exergy of working fluid mass flow, $\dot{EX}_{in}^{Q}$ is the input exergy and $\dot{EX}_{out}^{Q}$ is the work output, and $\dot{S}_{gen}$ represents the rate of entropy creation. Eqs. (9) and (10)

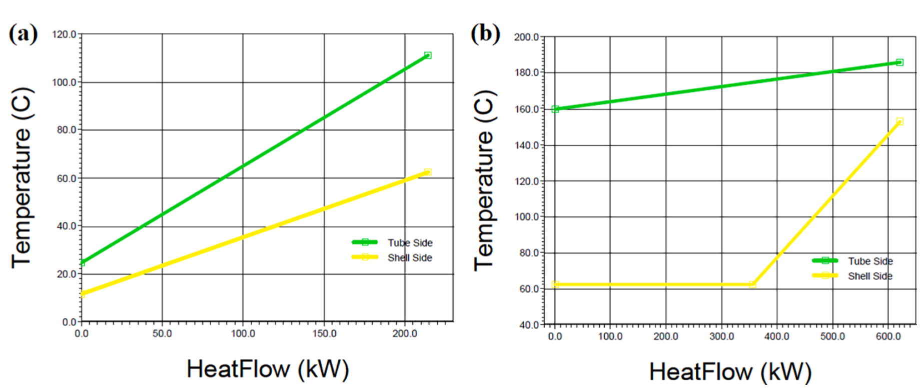

Fig. 4. Heat profile in biomass-ORC components: a) regenerator, b) evaporator.

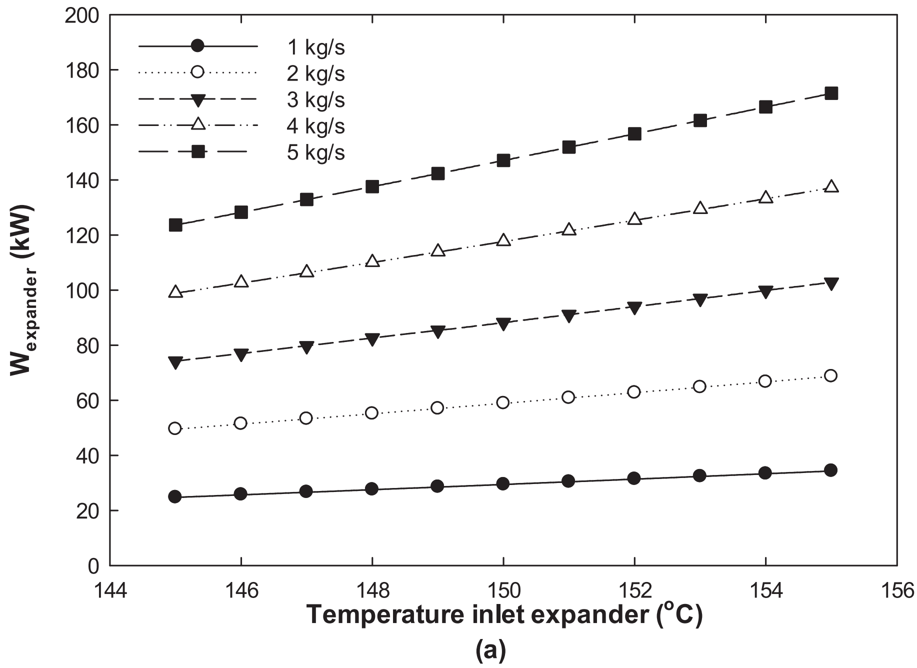

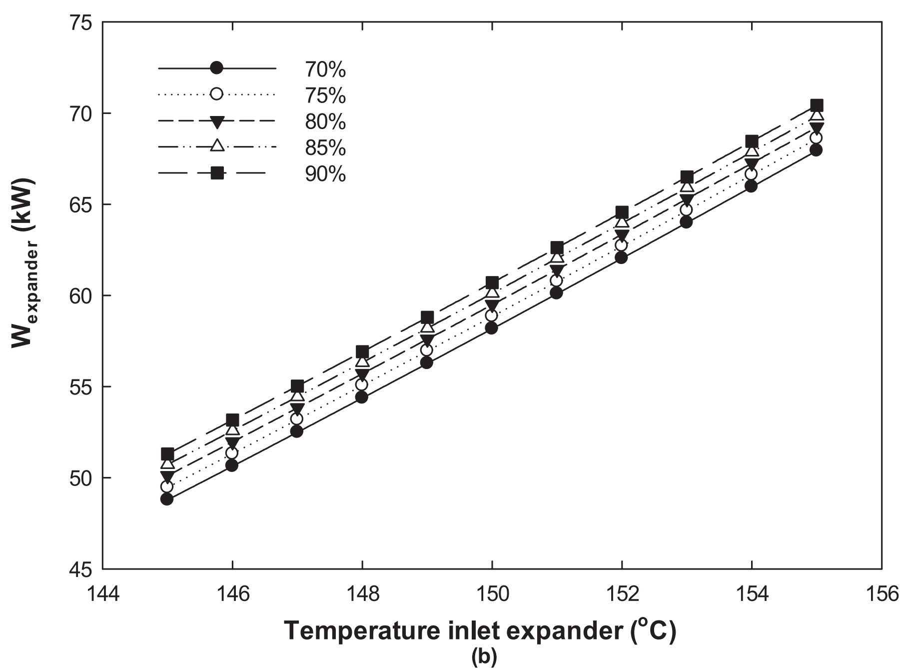

Fig. 5. The performance of $W_{expander}$ vs Temperature inlet expander in different variable: a) mass flow rate, b) isentropic efficiency, c) evaporator pressure.

express the thermomechanical exergy flow [34]:

$$i = \sum_{in} \dot{m}_{ex} - \sum_{out} \dot{m}_{ex} - \dot{EX}^{Q}_{in} - \dot{EX}^{Q}_{out} = T_0 \dot{S}_{gen} \tag{9}$$

$$e_x = h - h_0 - T_0 (s - s_o) \tag{10}$$

where h_0 is the specific enthalpy (kJ/kg) and s_0 is the spesific entropy (kJ/kg.K) at dead state pressure and temperature (P_0, T_0), which are 0.101325 Mpa (1 atm) and 5 °C, respectively.

$$\psi_{system} = \frac{\sum \dot{W}_{ORC}}{\dot{E}_{Xin}} \tag{11}$$

where ψ_{system} is the exergy efficiency of the system, it can be determine by eq. (11) [35]. $\dot{E}x_{in}$ is the inlet exergy is interpreted by eq. (14), As a result, the exergy destruction for each ORC component is indicated below:

Process 1–2, pump:

$$\dot{W}_{pump} = \dot{E}_{X1} - \dot{E}_{X2} + \dot{E}_{D\_pump}, \tag{12}$$

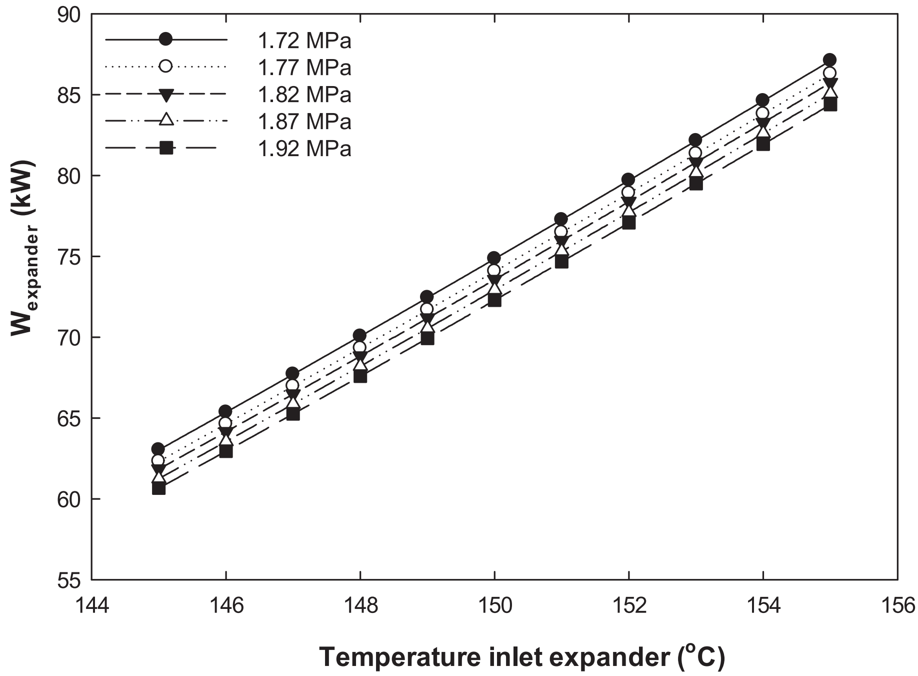

Fig. 5. (*continued*).

Process 2–3, regenerator:

$$\dot{E}_{D\_reg} = \dot{E}_{X2} + \dot{E}_{X2} - \dot{E}_{X3} - \dot{E}_{X6}, \tag{13}$$

Process 3–4, evaporator:

$$\dot{E}_{D\_evap} = \left(1 - \frac{T_0}{T_{in}}\right) Q_{in} + \dot{E}_{X3} - \dot{E}_{X4}, \tag{14}$$

Process 4–5, expander:

$$\dot{E}_{D\_exp} = \dot{E}_{X4} - \dot{E}_{X5} - \dot{W}_{exp}, \tag{15}$$

Process 6–1, condenser:

$$\dot{E}_{D\_cond} = \dot{E}_{X6} - \dot{E}_{X1} - \dot{Q}_{cond}, \tag{16}$$

$\dot{E}_{D\_expander}, \dot{E}_{D\_cond}, \dot{E}_{D\_evap}, \dot{E}_{Dpump}, \dot{E}_{D\_reg}$ are represent the destruction of exergy in the expander, condenser, pump, evaporator, and regenerator, respectively. Exergy analysis may improve economic and environmental performance by determining how much energy quality is accessible in biomass-ORC system. Furthermore, this study use the exergy function to measure the sustainability of a mechanism and system. It is also known as the exergy sustainability index (ESI) among academics. Among other things, ESI is a reliable indicator. Eqs. (17)–(20) access the degree of sustainability and may be determined from the related exergy balancing eqs for each cycle and study of ESI [36].

Exergy waste ratio (EWR):

$$EWR = \frac{\sum \dot{E}_{Xwaste}}{\sum \dot{E}_{Xinput}} = \frac{\sum \dot{E}_{destroyed}}{\sum \dot{E}_{Xinput}}; \tag{17}$$

Exergy efficiency:

$$\psi_{overall} = \frac{\dot{E}_{Xout}}{\dot{E}_{Xin}}; \tag{18}$$

Environmental effect factor (EEF):

$$EEF = \frac{EWR}{\psi_{overall}} \tag{19}$$

Exergy sustainability index (ESI):

$$ESI = \frac{1}{EEF}. \tag{20}$$

This analysis is conduct with some presumptions: 1) steady state, 2) heat losses and pressure drop in component systems are neglected, 3) inlet expander temperature was based on a variation of $T_{c,o}$, 4) the cooling water temperature is set at 25 °C, 5) the pump and expander isentropic efficiency was set at 65 % and 70 %, respectively, 6) the exergy of hot water from the evaporator and the exergy of cooling water that entering and leaving a condenser are neglible.

Economy analysis

Thermoeconomics seeks to determine the cost formation process of internal flows and ultimate products in energy systems and process plants [37]. This allows for a more accurate assessment of the various production possibilities and a better knowledge of the internal economic processes that occur during the production process. The word thermoeconomics refers to a mix of thermodynamic and economic analysis. Exergoeconomics is distinguished by the specific application of exergy in thermodynamic analysis. As a result, thermoeconomics, as a more broad term, can be used in place of exergoeconomics, but not vice versa [38]. The proposed approach incorporates energy into thermodynamic analysis and reflects the unit costs of flows in an energy base. There were two key reasons for using energy rather than exergy in the computations. First, unit charges in terms of energy are the most common billing system viewed by final customers, who will ultimately decide whether or not to employ the solar plant's energy services (consumers pay per unit of energy consumed). Second, there is no cost allocation (each component has a single product flow) [39].

Thee economic indicators used in the analysis are Simple Pay Back (SPB), Net Present Value (NPV), and levelized cost of electricity (LCOE) (Eqs. (21)–(23).

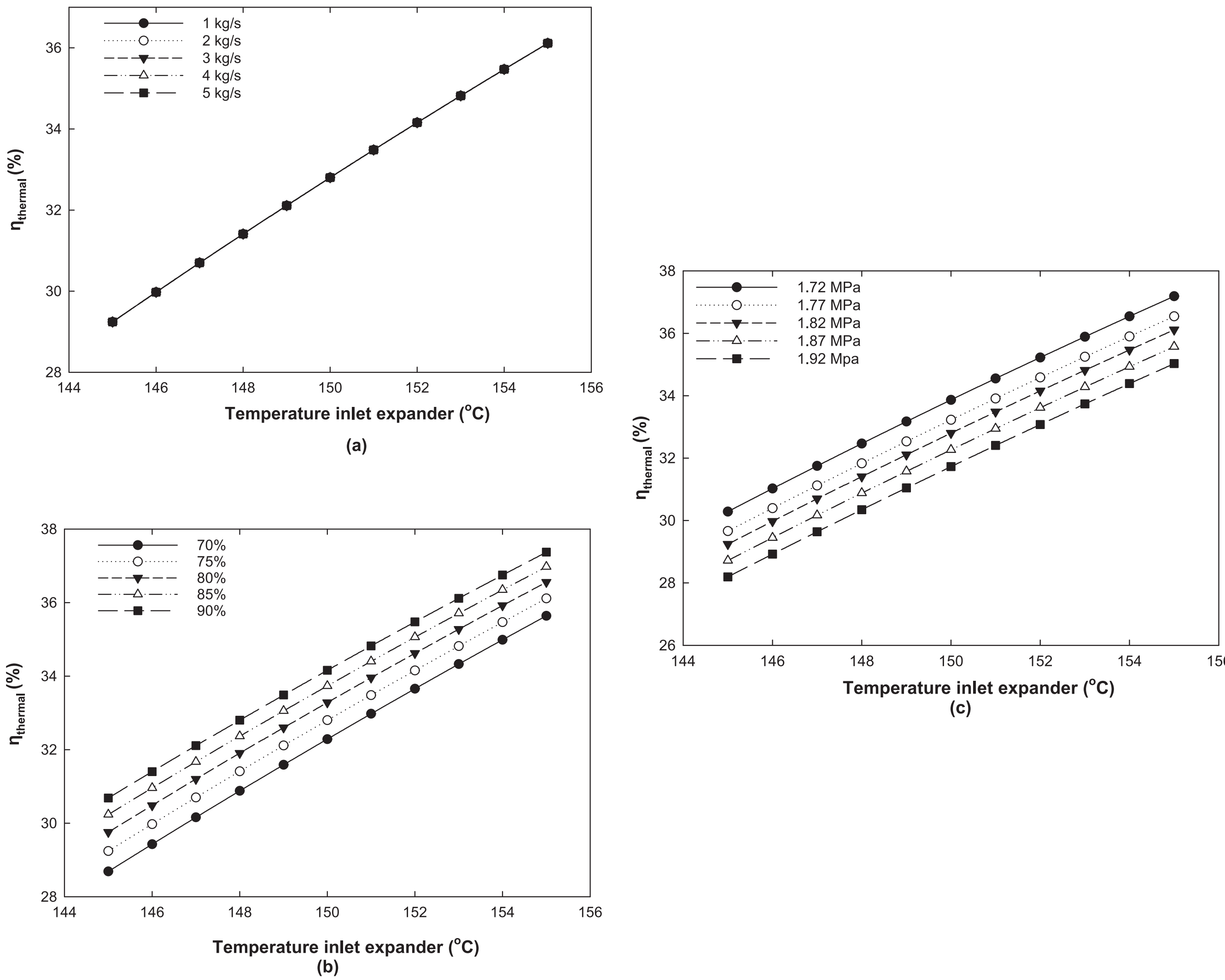

Fig. 6. The performance of $\eta_{thermal}$ vs temperature inlet expander in different variable: a) mass flow rate, b) isentropic efficiency, c) evaporator pressure.

$$SPB = \frac{C_{TCI}}{C_{ncf}} \tag{21}$$

$$NPV = -(C_{TCI}) + \sum_{i=1}^{N} C_{ncf}(1+i)^{-t} \tag{22}$$

$$LCOE = \frac{\frac{C_{TCI}}{1-(1+i)^{-n}} + (C_{bio} + C_{ash} + C_{O\&M})}{E_{e,a}} \tag{23}$$

where C_{TCI} represent the system's total capital investment, to calculate it, add the beginning costs of the system's components, as stated in Eq. (24) and Table 3 shows the breakdown cost equations of each components for ORC system. C_{ncf} is the system's annual economic savings, determined by adding annual revenues and operational costs (Eq. (25)).

$$C_{TCI} = C_{Boiler} + 1.5C_{ORC,PEC} \tag{24}$$

$$C_{ncf} = (C_e + C_h) - (C_{bio} + C_{ash} + C_{O\&M}) \tag{25}$$

where $C_e, C_h, C_{bio}, C_{ash}, C_{O\&M}$ is annual selling electricity cost, annual selling heating cost, annual biomass consumption, annual disposal ash, and annual cost operational and maintenance, respectivelly. Several approaches are used in the literature to calculate the entire cost of ORC systems based on the acquired equipment cost, taking into account extra expenses like as installation labour, piping, instrumentation and controls, electrical equipment, structural work, engineering, and supervision. In the current analysis, the assumed split of these expenses is provided in Table 4.

The particular investment cost (€/kWe), which expresses the investment cost per unit of installed electrical capacity, is thus defined as the following equation:

$$SIC = \frac{C_{TCI}}{W_{net,plant}} \tag{26}$$

The economic assumptions are summarized in Table 5. The price of biomass is an important factor in determining the investment's cost-effectiveness. However, its value is highly unknown because it is determined by a variety of global and local factors, including the type and quality of biomass, availability, supply and demand, internationally and nationally adopted bioenergy legislation, supply chains, and so on.

The EU has a number of assistance schemes in place to encourage the use of biomass to generate electricity. According to existing feed-in-tariff schemes, power selling prices from solid biomass vary in different EU member states from a minimum of 81.2 €/MWhe (Slovakia) to up to 198 €/MWhe (Italy), with the majority falling between 90 and 120 €/MWhe [45]. The selling price of energy is determined by national regulation. It may vary depending on the plant's power capacity and scope, with smaller plants and combined heat and power units being more heavily incentivized. As a result, in the current work, a base-case value of 120 €/MWhe is assumed. This analysis estimates a base-case value of 0.065

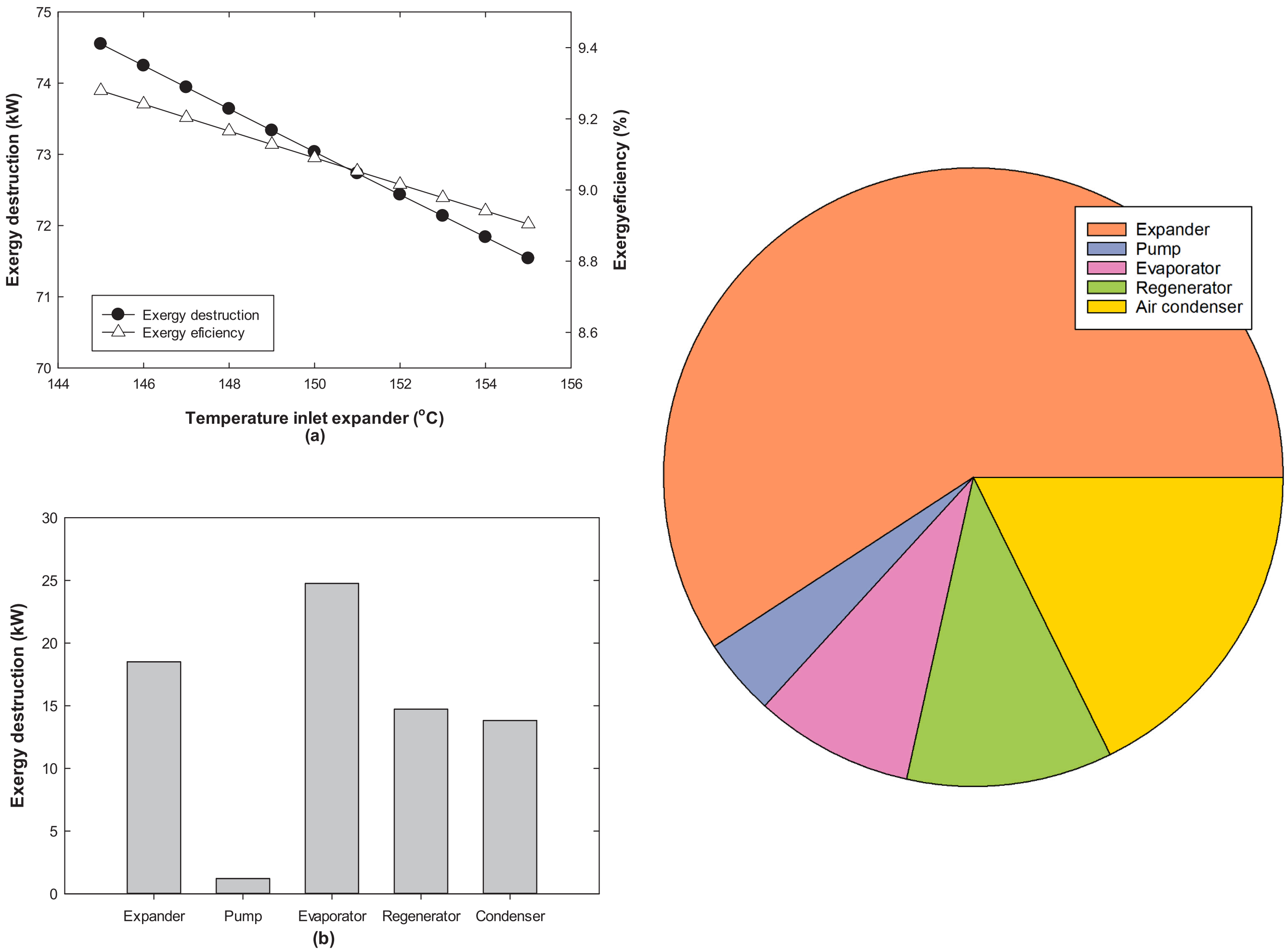

Fig. 7. Exergy performance of biomass-ORC: a) temperature inlet expander, b) components exergy destruction, c) exergy efficiency of each components.

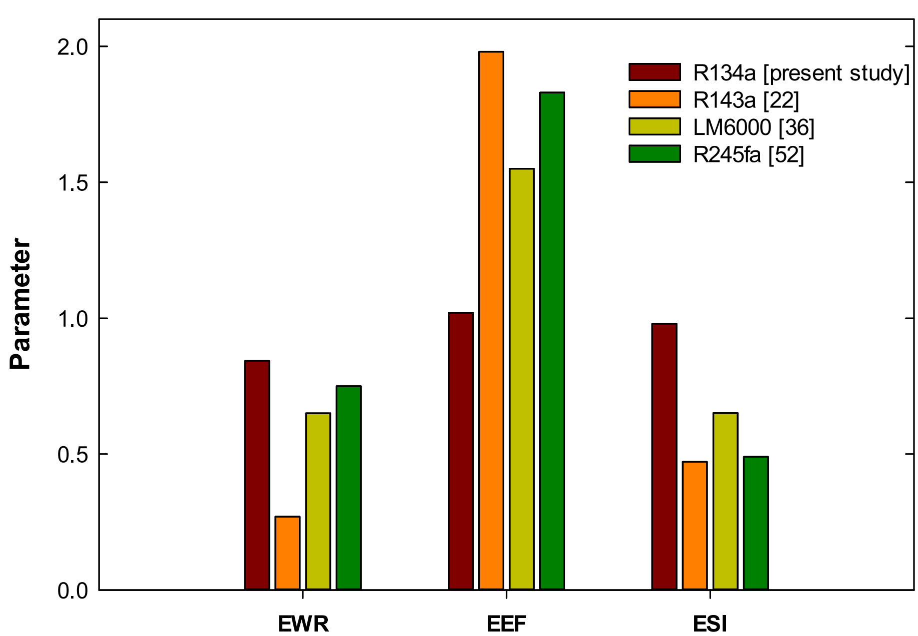

Fig. 8. Exergy sustainability indicators.

Table 8
Component's invesments cost.

Components	Investment cost
Boiler (k€)	1,684
Expander (k€)	135
Pump (k€)	9.2
Evaporator (k€)	18.9
Regenerator (k€)	24.6
Air-cooled condenser (k€)	40.4
Working fluid (€)	75
O&M (k€)	38.2
C_e (k€/year)	28.5
C_h (k€/year)	169.4
C_{bio} (k€/year)	75
C_{ncf} (k€)	84.4

Table 9
Annual economic biomass-ORC plant.

Parameter	Present value	Value [44]
C_{TCI} (k€)	2025	1224
SIC_{Plant} (k€/kWe)	13.5	13.9
SIC_{ORC} (k€/kWe)	2.3	2.4
NPV (k€)	238	259
SPB (years)	24	20
LCOE (€/kWh)	0.93	0.91

€/kWh.

Results and discussion

This chapter will discuss the study results of the parametric analysis, energy, optimization and exergy calculations from the biomass-ORC analysis using the equations in the previous chapter and include the several literatures to strengthen the results of the analysis. Table 6 shows the main parameter and assumption that used in this study.

Model validation

After each component has been correctly modelled and merged into a unified system capable of iteration, the analysis tool's final schematic diagram is generated. The cooling tower and condenser's condition determines whether or not the two pieces of equipment can operate correctly. Once the biomass-ORC system model is operational, check the data from the modelling findings and the system's actual operating circumstances, as stated in Table 7. The modelling settings show a significant variance in pump power and regenerator temperature, with 1 and 2 % differences, respectively. There is quite a large difference in pump power and condenser evaporator, with 4 % differences error, respectively. This is because several parameters are not known in actual conditions, such as the properties of moist air, the size of the air condenser and regenerator sizing, which can affect the temperature of the working fluid that enters the pump and that will be heated in the regenerator. To simplify the system performance simulation in the current study, the assumptions are as follows: 1) The process from the producing biomass stream to the ORC plant functions under steady-state condition. (2) The biomass stream is considered to be pure water for calculating thermodynamic characteristics. 3) The biomass-ORC plant neglected the pressure drop, heat loss, and changes in kinetic and potential energy. 4) The composition of the working fluids and mixes remains constant during operation. 5) The temperature dead state (T_0) and pressure dead state (P_0) in the Bologna biomass-ORC field are 5 °C and 1 atm.

Fig. 4 is a profile of the heat exchanger (regenerator and evaporator) used in the biomass-ORC plant in Bologna. It can be seen in Fig. 4a, where the regenerator plays a role in the initial heating due to heat transfer flow from the expansion of the expander (green line) so that the working fluid from the pump (yellow line) can be heated until the temperature increases ~ 50 °C with the heat of 220 kW so that the condenser load to cool the working fluid is not excessive. Next, Fig. 4 b shows the heat transfer from the biomass stream (green line) and working fluid (yellow line) in the evaporator, where the working fluid from the regenerator can be heated to 155 °C with a heat supply of 620 kW. So that the temperature and heat possessed by the working fluid are sufficient to rotate the expander and produce electricity.

Parametric analysis

Fig. 5 shows the performance of the $W_{expander}$ against increasing temperature with different variables (mass flow rate, isentropic efficiency, and evaporator pressure). Fig. 5a shows the difference in mass flow rate (1–5 kg/s) and temperature rise (145–155 °C) on the size of the $W_{expander}$. We can see that the greater the mass flow rate, the greater the power produced, assuming that the pipe sizing follows a significant mass flow rate so that a mass flow rate of 5 kg/s produces the largest $W_{expander}$ (171.5 kW) in the same evaporator temperature range (155 °C). The significant increase in $W_{expander}$ is shown in Fig. 5b, where the isentropic efficiency increases (0.7–0.9) in both pumps and expanders. The isentropic efficiency increase in components results in minor losses produced by the components, so energy conversion isoptimal. Using the isentropic efficiency assumption of 0.9 results in an expander size of 70.43 kW in the same temperature range. On the other hand, Fig. 5c shows the difference in evaporator pressure (1.72–1.87 MPa) as the resulting $W_{expander}$ increases, where the smallest evaporator pressure value (1.72 MPa) produces the largest $W_{expander}$ (87.1 kW) in the same temperature range. This is because the power required by the pump is smaller (3.23 kW), and the heat produced by the evaporator is more optimal (225.5 kW) to produce greater enthalpy for use by the expander in the same temperature range.

Similar results are shown in Fig. 6, where there is an increase in temperature on the thermal efficiency of biomass-ORC. In Fig. 6a, changes in mass flow rate (1–5 kg/s) do not significantly affect efficiency because the difference in net power is only affected by the increase in temperature. This differs from isentropic efficiency, where the difference between W_{net} and evaporator heat is greatly influenced by isentropic efficiency. So, the highest isentropic efficiency value (0.9) produces the highest thermal efficiency (37.4 %) at the same temperature. The thermal efficiency results in Fig. 6c produce the same trend as Fig. 5c, where the lowest evaporator pressure (1.72 MPa) produces the highest thermal efficiency with a value of 37.2 %.

In the analysis results in Fig. 5a and 6a, increasing the mass flow rate only has a significant effect on expander power but tends to stagnate on the efficiency of the ORC system. This was experienced by research by Soltani et al. [49], where increasing the mass flow-rate typically enhances all extensive outputs, which is expected as a result of increased power generation. While, varying the fuel mass flow rate has no effect on system's efficiency (since only capacity increases). Meanwhile, research by Korelas et al. [50] confirms the results of the increase in expander power and system efficiency as the expander inlet temperature increases (Fig. 5c and 6c). It shows that lower pressure at high temperatures produces the highest expander power in biomass-ORC generation.

Exergy performance

This subchapter will discuss the effect of exergy on the system and its components. Fig. 7a shows the decrease in destruction exergy and system exergy efficiency as the expander inlet temperature increases, where the highest temperature (155 °C) produces the lowest destruction exergy and efficiency exergy with amounts of 71.54 kW and 8.9 %, respectively. Meanwhile, the highest exergy damage experienced by each component is the evaporator, and the lowest is the pump, with values of 24.76 and 1.2 kW, respectively as shown in Fig. 7b. The evaporator is also the most significant exergy-contributing component compared to other components, around 33.84 %, which can be seen in Fig. 7c. This is very natural because the evaporator is the component where heat exchange between the biomass heat source and the working fluid occurs, and an increase in entropy due to non-optimal heat conversion often occurs. In some literature, the exergy destruction value of the evaporator is very high, but this is minimized by a regenerator, which utilizes the heat from the expansion in the expander so that it is not directly cooled by the condenser so that the cooling load can be reduced.

Environmental analysis

Fig. 8 depicts the exergy sustainability of each working fluid, as indicated by numerical parameters such as exergy waste ratio (EWR), environmental effect factor (EEF), and exergy sustainability index (ESI), as well as two benchmarks for comparison. EWR is the ratio of overall waste exergy to overall input exergy, and according to the computation, practically all working fluids have almost the same EWR value, ranging from 0.25 to 0.85, with R134a having the highest EWR value of 0.843 and R143a having the lowest EWR value of 0.27 [22]. The EWR value is relatively minor in comparison to the studies done by Aydin [36] on the turbine component and Abam et al. [51] with the working fluid R245fa, which generate EWR values of 0.65 and 0.75, respectively.

Another indicator is the environmental effect factor, it may indicate the system's environmental harm caused by waste exergy destruction [51]. Fig. 8 displays the EEF values of each working fluid, with Propane having the highest EEF value of R143a [22], followed by R245fa [51], R134a with EEF values of 1.98, 1.83, and 1.02, respectively. R134a, on the other hand, had the lowest EEF value among working fluids and was regarded as more sustainable. The R134a had a lower environmental impact than other working fluids. As the last review, ESI is a degree of sustainability that serves as a supplement to the EEF [36]. Fig. 8 shows that R134a had the highest ESI value of 0.98. These values are relatively minor compared to Aydin [36] and Abam et al. [51], who had ESI values of 0.651 and 0.491, respectively.

Economic analysis

This section discusses the crucial findings from the case study system's economic analysis. Table 7 shows investment costs for the system's components. The total investment cost (C_{TCI}) is the sum of the individual system's components. While, Table 8 shows the annual economic analysis of the system including SIC, NPV, SPP, and LCOE.

Both tables are produced assuming the maximum power and temperature are 150 kWe and 160 °C, respectively. We can see from Table 8 that the highest costs of a biomass-based ORC generator are the components of processing biomass into fuel, where investment costs can be more than 60 % of the total investment in all biomass-ORC plants. Meanwhile, the cost of the ORC itself is the most expensive, namely the expander component, which is 135 k€. Because the expander or turbine components for the ORC generator have yet to be made en masse and in the conditions of the biomass-ORC field, they use components from scroll-type compressors, which are converted into the desired expander. Can cut investment costs. Meanwhile, T_{CTI} and C_{nf} are obtained from Eqs. (20) and (21) with the assumption that the average selling price of heating and electricity for the last three years is around 80–100 €/MWh and with biomass consumption of 1500 tons/year and assuming residential use of up to 2000 hr/year. So from these parameters, we get SIC, NPV and LCOE of 13.5 k€/kWe, 238 k€/year and 0.93 €/kWh, respectively (Table 9). This mean that investment in ORC with biomass is quite significant compared to conventional nuclear and coal fuel plants. Moreover, from the calculation results, SPB from biomass-ORC investment can be achieved in 26–27 years, assuming constant inflation. If we look at similar research conducted by Braimakis et al. [44] using cyclopentane working fluid, his simulation produces power and efficiency of around 88 kWe and 8.1 %, respectively. Table 8 shows several differences between the annual biomass-ORC economic calculations. This can be based on making different assumptions regarding component prices, net electricity selling prices, biomass prices, and annual energy usage hours.

Conclusion

A thermodynamic analysis was carried out to confirm how much power the Bologna ORC plant can get using biomass fuel. The study results found that under current conditions, only 85 kW can be generated by the site compared to the planned capacity (150 kWe). From the results of the optimization analysis, it was found that to obtain clean power and optimum system thermal efficiency of 149.56 kW and 13.77 %, a mass flowrate of 4.5 kg/s was required, an evaporator pressure of 1.84 MPa, a condenser pressure of 0.4 MPa and an expander inlet temperature of 152 °C. From the results of the exergy analysis, it was found that the evaporator and expander were the components that produced exergy damage to the system, with exergy damage rates of 33.84 % and 25.35 %, respectively. Furthermore, at a temperature of 155 °C, the results of the exergy sustainability indicators EWR, EEF, and ESI produce pretty good values, namely around 0.83, 1.05, and 0.89, respectively, which means that the Bologna biomass-ORC plant is quite feasible, environmentally friendly and has high sustainability index. Moreover, In terms of economic analysis, biomass-ORC investment is a reneable energy generation that is quite competitive, as seen from the NPV and LCOE values of 238 k€ and 0.93 €/kWh and a simple payback period of 24 years, assuming the resident's annual energy needs reach 2000 h/year.

CRediT authorship contribution statement

Diki Ismail Permana: Writing – original draft, Visualization, Software, Methodology, Investigation, Formal analysis, Data curation, Conceptualization. **Federico Fagioli:** Writing – review & editing, Validation, Project administration, Investigation. **Maurizio De Lucia:** Writing – review & editing, Validation, Supervision, Project administration. **Dani Rusirawan:** Writing – review & editing, Supervision, Project administration, Formal analysis, Conceptualization. **Istvan Farkas:** Writing – review & editing, Supervision, Resources, Formal analysis, Conceptualization.

Declaration of competing interest

The authors declare that they have no known competing financial interests or personal relationships that could have appeared to influence the work reported in this paper.

Data availability

Data will be made available on request.

Acknowledgements

The experimental activities on-field carried out on the biomass-ORC power plant are courtesy of the company Global Therm S.r.l. in the person of Sandro Bazzechi, CEO of the company, and Andrea Unicori, technical director.

References

[1] Terna Group Statistiche Regionali. ISTAT Database 2019. Available online: https://download.terna.it/terna/Statistiche%20Regionali_2018_8d7b93cbf9ad480.pdf (accessed on 1 July 2020).

[2] Viola M. The consequences of the Ukraine War on the energy sector in Italy. Retrieved from, https://eccoclimate.org/consequences-ukraine-war-on-the-energy-sector-in-italy/; 2024.

[3] https://www.trade.gov/country-commercial-guides/italy-natural-gas-renewable-energy.
[4] Statista Research Department. 2020. Available online: https://www.statista.com/markets/421/topic/496/forestry/ (accessed on 1 July 2020).
[5] Commission E. Directive 2001/77/EC of the European Parliament and of the Council of 27 September 2001 on the promotion of electricity produced from renewable energy sources in the internal electricity market. O J Eur Union 2001; 283:33–40.
[6] European Commission. Eurostat. Available online: https://ec.europa.eu/eurostat (accessed on 15 June 2020).
[7] Fiper. Teleriscaldamento a Biomassa: Un Investimento Per il Territorio; Srl, R.A.G., Ed.; 2018; ISBN 9788894343700. Available online: http://www.fiper.it/fileadmin/user_upload/biblioteca/libroFIPER-teleriscaldamento-abiomassa un-investimento-per-il-territorio.pdf (accessed on 1 July 2020).
[8] Ricerca Sistema Energetico. Energia Dalle Biomasse Legnose. Ricerca Sistema Energetico: Milano, Italy; 2019.
[9] Gunawan G, Permana DI, Soetikno P. Design and numerical simulation of radial inflow expander of the regenerative brayton cycle using supercritical carbon dioxide. Res Eng 2023;17:100931. https://doi.org/10.1016/j.rineng.2023.100931.
[10] Carraro G, Bori V, Lazzaretto A, Toniato G, Danieli P. Experimental investigation of an innovative biomass-fired micro-ORC system for cogeneration applications. Renew Energy 2020;161:1226–43. https://doi.org/10.1016/j.renene.2020.07.012.
[11] Roy D, Samanta S, Ghosh S. Performance assessment of a biomass fuelled advanced hybrid power generation system. Renew Energy 2020;162:639–61. https://doi.org/10.1016/j.renene.2020.07.030.
[12] Parvez M, Khan O. Parametric simulation of biomass integrated gasification combined cycle (BIGCC) power plant using three different biomass materials. Biomass Convers Biorefin 2019;10(4):803–12. https://doi.org/10.1007/s13399-019-00499-x.
[13] Nami H, Anvari-Moghaddam A, Nemati A. Modeling and analysis of a solar boosted biomass-driven combined cooling, heating and power plant for domestic applications. Sustainable Energy Technol Assess 2021;47:101326. https://doi.org/10.1016/j.seta.2021.101326.
[14] Braimakis K, Magiri-Skouloudi D, Grimekis D, Karellas S. Energy-exergy analysis of ultra-supercritical biomass-fuelled steam power plants for industrial chp, district heating and cooling. Renew Energy 2020;154:252–69. https://doi.org/10.1016/j.renene.2020.02.091.
[15] Salvestroni M, Pierucci G, Pourreza A, Fagioli F, Taddei F, Messeri M, et al. Design of a solar district heating system with seasonal storage in Italy. Appl Therm Eng 2021;197:117438. https://doi.org/10.1016/j.applthermaleng.2021.117438.
[16] Kristyadi T, Permana DI, Sirodz MP, Saefudin E, Farkas I. Performance and emission of diesel engine fuelled by commercial bio-diesel fuels in Indonesia. Acta Technologica Agriculturae 2022;25(4):221–8. https://doi.org/10.2478/ata-2022-0032.
[17] Gimelli A, Luongo A. Thermodynamic and experimental analysis of a biomass steam power plant: Critical issues and their possible solutions with CCGT systems. Energy Procedia 2014;45:227–36. https://doi.org/10.1016/j.egypro.2014.01.025.
[18] Permana DI, Rusirawan D, Farkas I. A bibliometric analysis of the application of solar energy to the organic rankine cycle. Heliyon 2022;8(4). https://doi.org/10.1016/j.heliyon.2022.e09220.
[19] Permana DI, Rusirawan D, Farkas I. The theoretical approach of the solar organic rankine cycle integrated with phase change material for the Hungarian region. Energy Sci Eng 2023;11(12):4429–45. https://doi.org/10.1002/ese3.1589.
[20] De Lucia M, Pierucci G, Manieri M, Agostini G, Giusti E, Salvestroni M, et al. Experimental characterization of commercial scroll expander for micro-scale solar Orc application: part 1. Energies 2024;17(9):2205. https://doi.org/10.3390/en17092205.
[21] Taccani R, Obi JB, De Lucia M, Micheli D, Toniato G. Development and experimental characterization of a small scale solar powered organic Rankine cycle (ORC). Energy Procedia 2016;101:504–11. https://doi.org/10.1016/j.egypro.2016.11.064.
[22] Permana D, Rusirawan D, Farkas I. Waste heat recovery of Tura geothermal excess steam using organic Rankine cycle. Int J Thermodyn 2021;24(4):32–40. https://doi.org/10.5541/ijot.906128.
[23] Permana DI, Sutikno P. Numerical simulation of turboexpander on organic Rankine cycle with different working fluids. IOP Conference Series: Materials Science and Engineering 2019;694(1):012014. https://doi.org/10.1088/1757-899x/694/1/012014.
[24] Tartiere T, Marco A. September). ORC World Map: Organic Rankine Cycle World Map; 2018. https://orc-world-map.org/.
[25] Georgousopoulos S, Braimakis K, Grimekis D, Sotirios Karellas S. Thermodynamic and techno-economic assessment of pure and zeotropic fluid ORCs for waste heat recovery in a biomass IGCC plant. Appl Therm Eng 2021;183:116202.
[26] Zhang C, Shu G, Tian H, Wei H, Liang X. Comparative study of alternative ORC-based com-bined power systems to exploit high temperature waste heat. Energy Convers Manag 2015;89:541–54.
[27] Moharamian A, Soltani S, Rosen MA, Mahmoudi SMS, Morosuk T. A comparative thermoeco-nomic evaluation of three biomass and biomass-natural gas fired combined cycles using organic Rankine cycles. J Clean Prod 2017;161:524–44.
[28] Oyekale J, Heberle F, Petrollese M, Brüggemann D, Cau G. Biomass retrofit for existing solar organic Rankine cycle power plants: Conceptual hybridization strategy and techno-economic assessment. Energy Convers Manag 2019;196: 831–45.
[29] Sadeghi S, Askari IB. Prefeasibility techno-economic assessment of a hybrid power plant with photovoltaic, fuel cell and Compressed Air Energy Storage (CAES). Energy 2019;168:409–24. https://doi.org/10.1016/j.energy.2018.11.108.
[30] Bai Z, Liu Q, Lei J, et al. Investigation on the mid-temperature solar thermochemical power generation system with methanol decomposition. Appl Energy 2018;217(2018):56–65. https://doi.org/10.1016/j.apenergy.2018.02.101.
[31] Lemmon E, Huber M, McLinden M. NIST Standard Reference Database 23: Reference Fluid Thermodynamic and Transport Properties-REFPROP. Gaithersburg, MD, USA,.: National Institute of Standards and Technology:; 2013. Version 9.1;.
[32] Pala L, Wang Q, Kolb G, Hessel V. Steam gasification of biomass with subsequent syngas adjustment using shift reaction for syngas production: an Aspen Plus model. Renew Energy 2017;101:484e92.
[33] Moran MJ, Shapiro HN. Fundamental of Engineering Thermodynamics. 6th Ed. US: John and Wiley; 2008.
[34] Tchanche B, Lambrinos G, Frangoudakis A, Papadakis G. Exergy analysis of micro-organic rankine power cycles for a small scale solar driven reverse osmosis desalination system. Appl Energy 2010;87(4):1295–306. https://doi.org/10.1016/j.apenergy.2009.07.011.
[35] Yuksel YE, Ozturk M, Dincer I. Thermodynamic performance assessment of a novel environmentally-benign solar energy based integrated system. Energy Convers Manag 2016;119:109–20. https://doi.org/10.1016/j.enconman.2016.04.040.
[36] Aydin H. Exergetic sustainability analysis of LM6000 gas expander power plant with steam cycle". Energy 2013;57:766–74. https://doi.org/10.1016/j.energy.2013.05.018.
[37] Lozano MA, Valero A. Theory of the exergetic cost. Energy 1993;18(9):939–60. https://doi.org/10.1016/0360-5442(93)90006-y.
[38] Tsatsaronis G. Definitions and nomenclature in exergy analysis and exergoeconomics. Energy 2007;32(4):249–53. https://doi.org/10.1016/j.energy.2006.07.002.
[39] Pina EA, Lozano MA, Hernandez A, Lazaro A. Design and thermoeconomic analysis of a solar parabolic trough – orc – biomass cooling plant for a commercial center. Sol Energy 2021;215:92–107. https://doi.org/10.1016/j.solener.2020.11.080.
[40] Taheri MH, Mosaffa AH, Farshi LG. Energy, Exergy and economic assessments of a novel integrated biomass based multigeneration energy system with hydrogen production and LNG regasification cycle. Energy 2017;125:162–77. https://doi.org/10.1016/j.energy.2017.02.124.
[41] Fraia SD, Shah M, Vanoli L. A biomass-based polygeneration system for a historical building: A techno-economic and environmental analysis. Energy Convers Manage 2023;291:117336. https://doi.org/10.1016/j.enconman.2023.117336.
[42] Langdon, D. and Davis Langdon Engineering Services (2009) *Spon's mechanical and electrical services price book 2010* [Preprint]. doi:10.1201/9781482285505.
[43] Lemmens S. Cost engineering techniques and their applicability for cost estimation of organic rankine cycle systems. Energies 2016;9(7):485. https://doi.org/10.3390/en9070485.
[44] Braimakis K, Charalampidis A, Karellas S. Techno-Economic Assessment of a small-scale biomass orc-chp for district heating. Energy Convers Manage 2021;247: 114705. https://doi.org/10.1016/j.enconman.2021.114705.
[45] Banja M, Sikkema R, Jégard M, Motola V, Dallemand J-F. Biomass for energy in the EU – the support framework. Energy Policy 2019;131:215–28. https://doi.org/10.1016/j.enpol.2019.04.038.
[46] Pantaleo AM, Camporeale S, Fortunato B. Small scale biomass CHP: Techno-economic performance of steam vs gas turbines with bottoming orc. Energy Procedia 2015;82:825–32. https://doi.org/10.1016/j.egypro.2015.11.819.
[47] Pallis P, Gkonis N, Varvagiannis E, Braimakis K, Karellas S, Katsaros M, et al. Towards nzeb in Greece: A comparative study between cost optimality and energy efficiency for newly constructed residential buildings. Energ Buildings 2019;198: 115–37. https://doi.org/10.1016/j.enbuild.2019.06.005.
[48] Historical Data - News (n.d.). https://tradingeconomics.com/italy/electricity-price.
[49] Soltani R, Dincer I, Rosen MA. Thermodynamic analysis of a novel multigeneration energy system based on heat recovery from a biomass CHP cycle. Appl Therm Eng 2015;89:90–100. https://doi.org/10.1016/j.applthermaleng.2015.05.081.
[50] Karellas S, Braimakis K. Energy-Exergy Analysis and economic investigation of a cogeneration and trigeneration orc–VCC hybrid system utilizing biomass fuel and solar power. Energy Convers Manage 2016;107:103–13. https://doi.org/10.1016/j.enconman.2015.06.080.
[51] Abam FI, Ekwe EB, Effiom SO, Ndukwu MC, Briggs TA, Kadurumba CH. Optimum exergetic performance parameters and thermo-sustainability indicators of low-temperature modified organic Rankine Cycles (orcs). Sustainable Energy Technol Assess 2018;30:91–104. https://doi.org/10.1016/j.seta.2018.09.001.